also agrees with the seven-center 10 π-electron perimeter model discussed by Waluk and Michl and predicted earlier by Banister.[6] The separation Δ(HOMO) between the two highest occupied π MO's $2a_2$ and $3b_2$ is much less than separation Δ(LUMO) between $3a_2$ and $4b_2$. This has some significance for the detailed nature of the MCD term and is indeed consistent with Waluk and Michl's results. It is worthwhile emphasizing however that this excellent agreement is accomplished within the constraints of a single-determinant HFS scheme—a result counter to the position of Waluk and Michl that configuration interaction was essential for an adequate MO description of such systems.[11]

In addition to the electronic spectrum there is more general interest in $S_4N_3^+$ as a 10 π-electron system (cf. $S_3N_3^-$, $S_4N_4^{2+}$). The characteristics of the π bonding and indeed the overall bonding are relevant to interpreting the stability and the reactions of this cation, e.g. in scission[12] etc. Consequently, in Figure 1 we have provided the total overlap populations and charges of the ground state.[13]

From Figure 1 it is clear that the charge associated with each center indicates the usual strongly polar SN bonds; there is, as a result, a deficiency of charge on the sulfide fragment relative to the rest of the cation. These charges are consistent with the NMR measurement on ^{15}N.[14] The overlap population for the sulfide link is depressed to only 0.43 compared to 0.64 or higher in the open-chain S_3N^-[15] or S_4N^-[16] species but is comparable to that for the SS linkage in S_4N_2.[8c] In comparison to the SN bonds the SS bond is certainly weaker than either the S_aN_a or S_bN_a bonds and somewhat weaker than the S_bN_b link. This should be compared to S_4N_2 where the SN bond linking the S_3 portion to N_2S has the lowest overlap population and is indeed the point of scission. The overlap population of 0.50 for the S_bN_b bond is similar to that found in other π-electron-rich species (e.g., in $S_3N_3^-$[8c] it is 0.52) but is considerably less than in the cyclic dication $S_4N_4^{2+}$[9b] where the SN population is 0.61. The other SN bonds S_aN_a and S_bN_a are certainly quite strong with noticably enhanced overlap population of 0.71 and 0.72, respectively. In summary then, the total charges and overlap populations describe $S_4N_3^+$ as having strongly polar SN bonds, a weak sulfide single bond, a strong bond (roughly 1.5) between the sulfide and the rest of the molecule, and a SN single bond holding the unique nitrogen to its neighbors.

Some insight into these results can be gained by partitioning the overlap populations into π and σ contributions (by σ we denote those contributions that are symmetric to the molecular plane and include in this designation what are normally called σ bonds, "in-plane" p bonds, and lone pairs). In our calculations the π molecular orbitals belong to the a_2 and b_2 representations. As the entries in Figure 1 indicate, both the disulfide bond and the $S_bN_bS_b$ region have weak σ bonds (0.25 is roughly half a π bond) and also have only partial π-bond character (again 0.25 is roughly half a π bond). On the other hand, the large overlap populations of 0.71 and 0.72 for S_aN_a and S_bN_a bonds are a result of a full σ bond ($\sim$0.50) and a partial (half) π bond.

There is, of course, some variation in π-bond contribution around the ring (it is noticeably smaller in the disulfide bond), but it is clear that variations in bond strength in $S_4N_3^+$ can be attributed primarily to variations in the σ bond.

A more detailed analysis of calculated overlap populations reveals that is the orbitals $7a_1$ and $4b_1$ that are largely responsible for reducing the overlap in the S_bN_b and SS regions. They make antibonding overlap contributions of −0.055 and −0.074, respectively, to the S_bN_b and SS bonds. The "mechanism" of this destabilization can be illustrated by noting that in $4b_1$ there is a large self-atom population (or sulfur lone-pair character) of 0.44 that is carried in such a diffuse sulfur orbital that a strong antibonding interaction results with the neighboring nitrogen.

The 10 π electrons of $S_4N_3^+$ are distributed in orbitals that are essentially like those of a linear seven-center delocalized π system SNSNSNS, with the terminal sulfur folded back on one another. Thus, the first three π orbitals $1b_2$, $2b_2$, and $1a_2$ are clearly π bonding in the appropriate regions. However, the $3b_2$ and $2a_2$ π orbitals have both bonding and antibonding character depending on the region of the molecule. Indeed the π system is in some respects best interpreted as the strong interaction of four π electrons in a SS fragment (i.e., $\pi^2\pi^{*2}$) with six π electrons in a five-center NSNSN fragment (four π bonding and two nonbonding). This accounts for the depressed π-bonding character of the disulfide and the partial π bonds in the NS links.

The π orbitals $3b_2$, $2a_2$, $3a_2$, and $4b_2$ involved in the electronic transitions are of special interest. The overlap calculation indicates that the LUMO, $3a_2$, is primarily a disulfide orbital as are the HOMO − 1, $2a_2$, and HOMO − 2, $3b_2$. Consequently, the transitions $3b_2 \rightarrow 3a_2$ or $2a_2 \rightarrow 3a_2$ will weaken primarily the disulfide bond (especially in the case $3b_2 \rightarrow 3a_2$) but will have less effect on the remainder of the molecule. However, occupancy of the $4b_2$ orbital will weaken the $N_bS_bN_b$ region for both the $3b_2 \rightarrow 4b_2$ or $2a_2 \rightarrow 4b_2$ transitions and will weaken the disulfide only for the $3b_2 \rightarrow 4b_2$ transition.

In conclusion, the HFS calculation has allowed us to propose the identification of the molecular orbitals involved in the MCD spectrum. In addition, our results provide the basis for the analysis of both σ and π bonding in $S_4N_3^+$.

Acknowledgment. The calculations have been carried with a HFS program provided by Dr. T. Ziegler. We acknowledge operating grants from the NSERC (Canada) and CNPq (Brazil) (Contracts 30.0755/80 and 40.3107/82). The award of a Brazil/Canada scientific exchange grant to M.T. is also acknowledged.

Registry No. $S_4N_3^+$, 29631-23-0.

(11) The remark on this point in ref 6 may have been induced by the fact that Waluk and Michl are commenting on PPP calculations, a long way from the present ab initio results.
(12) A. J. Banister and N. R. M. Smith, *J. Chem. Soc., Dalton Trans.*, 973 (1980).
(13) R. S. Mulliken, *J. Chem. Phys.*, **23**, 1833 (1955).
(14) T. Chivers, R. T. Oakley, O. J. Schaer, and G. Wolmerhaüser, *Inorg. Chem.*, **20**, 914 (1981).
(15) J. Bojes, T. Chivers, W. G. Laidlaw, and M. Trsic, *J. Am. Chem. Soc.*, *104*, 4837 (1982).
(16) T. Chivers, W. G. Laidlaw, R. T. Oakley, and M. Trsic, *J. Am. Chem. Soc.*, **102**, 5773 (1980).

Contribution from the Solar Energy Research Group, The Institute of Physical and Chemical Research, Wako, Saitama 351, Japan

Optical Absorption and ESR Spectra of Monomeric Rhodium(II) Tetraphenylporphyrin in 2-Methyltetrahydrofuran Solution at 77 K

Mikio Hoshino,* Katsutoshi Yasufuku, Shiro Konishi, and Masashi Imamura

Received July 13, 1983

Rhodium porphyrins have aroused much attention because of the wide variety of their chemical reactions.[1] For instance, rhodium porphyrins readily react with the simple diatomic molecules H_2, O_2, and NO to produce hydride, oxygen, and

(1) Ogoshi, H.; Setsune, J.; Yoshida, Z. *J. Am. Chem. Soc.* **1977**, *99*, 3896–3870.

0020-1669/84/1323-1982$01.50/0

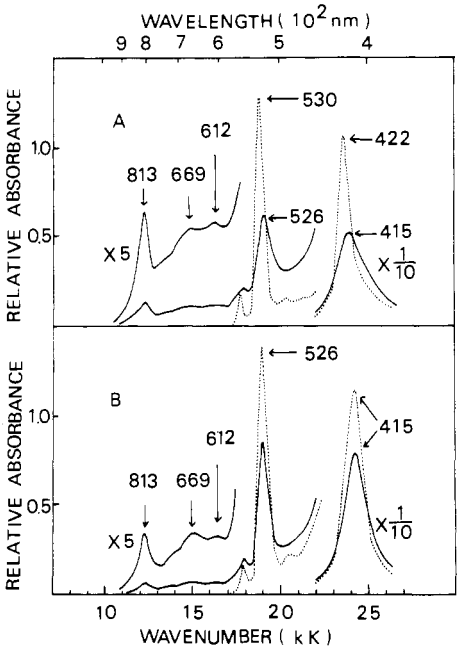

Figure 1. Optical absorption spectra of (A) ClRh^{III}TPP and (B) [Rh^{II}TPP]$_2$ in MTHF before (···) and after (—) UV irradiation for 1.0 h at 77 K.

nitric oxide adducts, respectively.[1-4]

The rhodium atom incorporated in porphyrin ligands is known to have three oxidation states, +1, +2, and +3. However, monomeric rhodium(II) porphyrins have neither been isolated nor detected spectroscopically because of their propensity to facile dimerization.[2] This note reports the optical absorption and ESR spectra of monomeric rhodium(II) tetraphenylporphyrin (Rh^{II}TPP) produced by photolysis of chloro(tetraphenylporphinato)rhodium(III) (ClRh^{III}TPP) and dimeric Rh^{II}TPP ([Rh^{II}TPP]^2) in 2-methyltetrahydrofuran (MTHF) solutions at 77 K.

Experimental Section

Crude ClRh^{III}TPP synthesized by the method reported by Sadasivan and Fleischer[5] was purified by column chromatography on alumina using dichloromethane as developer. The purified ClRh^{III}TPP was found to contain a small amount of the oxygen adduct, RhTPP(O_2), by the ESR measurement.[2] The MTHF solution of ca. 10^{-3} M ClRh^{III}TPP was degassed on a vacuum line prior to photolysis.

(μ-Tetraphenylporphinato)bis[dicarbonylrhodium(I)] (TPP[Rh^{I}(CO)$_2$]$_2$) was prepared according to the literature.[6] Dimeric Rh^{II}TPP ([Rh^{II}TPP]$_2$) was obtained by photolysis of TPP[Rh^{I}(CO)$_2$]$_2$ in degassed benzene solution according to eq 1 and 2,[7] where the products

$$\mathrm{TPP[Rh^{I}(CO)_2]_2} \xrightarrow{h\nu} \mathrm{Rh^{II}TPP + [Rh(0) + 4CO]} \quad (1)$$

$$\mathrm{2Rh^{II}TPP \rightarrow [Rh^{II}TPP]_2} \quad (2)$$

in brackets of reaction 1 are assumed stoichiometrically. Benzene of the photolyzed solution was replaced with MTHF on a vacuum line; the MTHF solution contains [Rh^{II}TPP]$_2$ on the order of 10^{-3} M. Chloro(tetraphenylporphinato)cobalt(III)[8] was kindly donated by Dr. K. Yamamoto of The Institute of Physical and Chemical Research. Benzene and MTHF were purified by fractional distillation and stored over Na–K alloy in vacuo in order to remove traces of water.

Absorption spectra were recorded on a Cary 14 spectrophotometer and X-band ESR spectra on a JEOL JES FE-3AX X-band spectrometer. Fields and frequencies were calibrated by Mn(II) in MgO powder and DPPH and a Takeda Riken TR 5501 frequency counter. The quartz optical cell used had an optical path length of 1.0 mm. Low-temperature photolysis was carried out by irradiating the solution in the optical cell or ESR tube immersed in liquid nitrogen; the light source was a high-pressure mercury lamp (Philips SP 500 W).

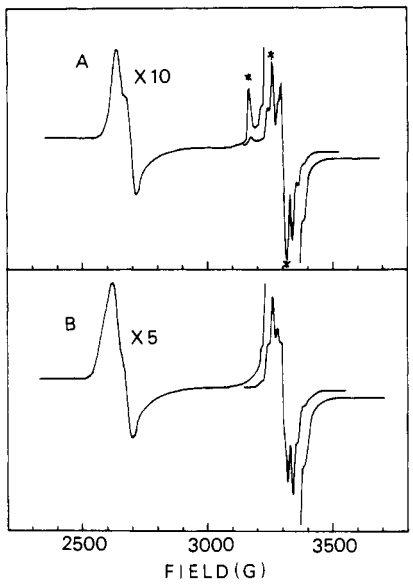

Figure 2. ESR spectra for UV-irradiated MTHF solutions of (A) ClRh^{III}TPP and (B) [Rh^{II}TPP]$_2$ at 77 K. The asterisks indicate the signals due to RhTPP(O_2).

Results and Discussion

Figure 1A shows the absorption spectra of ClRh^{III}TPP in MTHF solution at 77 K before and after irradiation with the mercury lamp for 1.0 h. The intensities of the absorption bands of ClRh^{III}TPP centered at 422 and 530 nm decrease with irradiation time, and new absorption bands appear at 415, 526, 612, 669, and 813 nm. The absorption spectrum obtained after 1 h of irradiation shows that ClRh^{III}TPP is almost completely photodecomposed. When the irradiated solution is warmed to room temperature and recooled to 77 K, the absorption peak at 526 nm becomes narrower than that measured before warming and the peaks at 612, 669, and 813 nm disappear.

Figure 1B shows the absorption spectra of [Rh^{II}TPP]$_2$ in MTHF solution at 77 K, measured before and after irradiation with the mercury lamp. The intensities of the 415- and 526-nm absorption bands decrease with the accompanying appearance of new absorption bands at 612, 669, and 813 nm. The resultant spectrum is identical with that observed for the irradiated ClRh^{III}TPP in MTHF solution as shown by solid lines in Figure 1. This fact implies that irradiation of both ClRh^{III}TPP and [Rh^{II}TPP]$_2$ in MTHF solutions at 77 K gives a common species, i.e., monomeric Rh^{II}TPP, as will be described later. The absorption bands that appeared by irradiation of [Rh^{II}TPP]$_2$ disappear upon warming to reproduce the original spectrum.

Figure 2A shows the ESR spectrum recorded for the irradiated MTHF solution of ClRh^{III}TPP at 77 K. The ESR spectrum observed for the solution prior to irradiation showed the presence of a small amount of RhTPP(O_2).[1] Since no

(2) Wayland, B. B.; Newman, A. R. *J. Am. Chem. Soc.* **1979**, *101*, 6472–6473.
(3) Wayland, B. B.; Newman, A. R. *Inorg. Chem.* **1981**, *20*, 3093–3097.
(4) Wayland, B. B.; Woods, B. S.; Pierce, R. *J. Am. Chem. Soc.* **1982**, *104*, 302–303.
(5) Sadasivan, N.; Fleischer, E. *J. Inorg. Nucl. Chem.* **1968**, *30*, 591–601.
(6) Ogoshi, H.; Setsune, J.; Omura, T.; Yoshida, Z. *J. Am. Chem. Soc.* **1975**, *97*, 6461–6466.
(7) Yamamoto, S.; Hoshino, M.; Yasufuku, K.; Imamura, M. *Inorg. Chem.* **1984**, *23*, 195–198.
(8) Sakurai, T.; Yamamoto, K.; Naito, H.; Nakamoto, N. *Bull. Chem. Soc. Jpn.* **1976**, *49*, 3042–3046.

signal is observed in the magnetic fields lower than 2900 G for the solution prior to irradiation, the ESR spectrum observed around 2650 G ($g = 2.46$) is ascribed to the photoproduct from $ClRh^{III}TPP$ at 77 K; the signal cannot be ascribed to any organic radical. Taking into account the $g_\perp$ values of 2.4-2.5[9,10] for rhodium(II) complexes with axial symmetry, we conclude that the signal is assigned to the perpendicular components of the monomeric $Rh^{II}TPP$. Owing to heavy background absorption due to $RhTPP(O_2)$ and solvent radicals produced by irradiation with the mercury lamp, we could not determine the $g_\parallel$ value of $Rh^{II}TPP$, which is expected to be nearly 2.0. The ESR signal vanishes when the irradiated solution is warmed to room temperature and recooled to 77 K. This is in accord with the fact that $Rh^{II}TPP$ readily dimerizes to form the diamagnetic dimer, $[Rh^{II}TPP]_2$.[2,7]

Figure 2B shows the ESR spectrum measured for the irradiated MTHF solution of $[Rh^{II}TPP]_2$ at 77 K. The irradiated solution shows the ESR signal at 2650 G, which is almost identical with that observed for the irradiated MTHF solution of $ClRh^{III}TPP$, indicating that the species giving rise to the spectrum is $Rh^{II}TPP$. No half-field signal is observed for the irradiated solution. The ESR signal disappears completely upon warming the irradiated solution to room temperature.

Rhodium(III) in $ClRh^{III}TPP$ is known to have a low-spin d^6 electronic configuration similar to cobalt(III) in $ClCo^{III}TPP$. We, therefore, preformed low-temperature photolysis of $ClCo^{III}TPP$ in MTHF at 77 K for comparison and found an ESR spectrum that is identical with that of authentic $Co^{II}TPP$.

Wavelength dependence on the photochemical reactions of $ClRh^{III}TPP$ and $[Rh^{II}TPP]_2$ was investigated by using cutoff filters. Optical and ESR measurements of the irradiated solutions revealed that $ClRh^{III}TPP$ and $[Rh^{II}TPP]_2$ form $Rh^{II}TPP$ with the irradiation light of $\lambda < 400$ nm and $\lambda < 310$ nm, respectively. No photochemical reaction was observed for the Q-band excitation of $ClRh^{III}TPP$ and $[Rh^{II}TPP]_2$ in MTHF solutions at 77 K.

Solvent radicals as well as $Rh^{II}TPP$ are the photoproducts from the irradiation of MTHF solutions of $ClRh^{III}TPP$ and $[Rh^{II}TPP]_2$. Since the irradiation of neat MTHF with the mercury lamp at 77 K gives rise to the formation of the solvent radicals, we consider that MTHF molecules absorbing UV light undergo C-H bond cleavage to produce a solvent radical (MTHF·) and an atomic hydrogen

$$MTHF \xrightarrow{h\nu} MTHF\cdot + H\cdot$$

followed by

$$MTHF + H\cdot \rightarrow MTHF\cdot + H_2$$

The major amount of the solvent radicals in the irradiated MTHF solutions of $ClRh^{III}TPP$ and $[Rh^{II}TPP]_2$ are presumed to be formed according to the above reaction scheme.

The irradiation of $ClRh^{III}TPP$ in an MTHF solution was performed with a cutoff filter transmitting the light of $\lambda > 360$ nm. Although this filter prevented the formation of solvent radicals from neat MTHF, the irradiated MTHF solution of $ClRh^{III}TPP$ exhibited ESR signals due to solvent radicals and $Rh^{II}TPP$. The photochemical formation of $Rh^{II}TPP$ from $ClRh^{III}TPP$ is assumed to be represented as

$$ClRh^{III}TPP \xrightarrow{h\nu\ (\lambda < 400\ nm)} Cl\cdot + Rh^{II}TPP$$

$$Cl\cdot + MTHF \rightarrow MTHF\cdot + HCl$$

The monomeric $Rh^{II}TPP$ is trapped stably in the MTHF matrix because of the high viscosity of the solvent at 77 K.

The Cl-Co homolytic cleavage also takes place at 77 K for $ClCo^{III}TPP$

$$ClCo^{III}TPP \xrightarrow{h\nu} Cl\cdot + Co^{II}TPP$$

followed by hydrogen abstraction of Cl· from an MTHF molecule. This homolytic cleavage may be justified from similar photoelimination of Cl· at 77 K frequently observed for benzyl chloride, $C_6H_5CH_2Cl$ and its derivatives in organic solvents:[11]

$$C_6H_5CH_2Cl \xrightarrow{h\nu} Cl\cdot + C_6H_5CH_2\cdot$$

The photochemical formation of $Rh^{II}TPP$ from $[Rh^{II}TPP]_2$ is considered to involve the fission of the Rh-Rh bond at 77 K:

$$[Rh^{II}TPP]_2 \xrightarrow{h\nu\ (\lambda < 310\ nm)} 2Rh^{II}TPP$$

Owing to the high viscosity of the solvent at 77 K, the resulting two $Rh^{II}TPP$ molecules, each of which has an unpaired electron, are expected to be located in close proximity; however, slight displacement of the two $Rh^{II}TPP$ molecules is presumably enough for each electron to be isolated electronically and magnetically. The solvent radicals observed in the irradiated solution are produced by photolysis of MTHF molecules, which absorb the light of $\lambda < 260$ nm. It should be noted that photodissociation of some organic dimers occurs readily in low-temperature matrices,[12-15] as in the present case.

Registry No. $Rh^{II}TPP$, 38856-19-8; $ClRh^{III}TPP$, 77944-60-6; $[Rh^{II}TPP]_2$, 88083-37-8.

(9) Shock, J. R.; Rogers, M. T. *J. Chem. Phys.* **1975**, *62*, 2640-2645.
(10) Muniz, R. P. A.; Vugman, N. V.; Danon, J. *J. Chem. Phys.* **1971**, *54*, 1284-1288.
(11) Porter G.; Strachan, E. *Trans. Faraday Soc.* **1958**, *54*, 1595-1604.
(12) Shida T.; Kira, A. *J. Phys. Chem.* **1969**, *73*, 4315-4320.
(13) Yamamoto, S.; Grellman, K. H. *Chem. Phys. Lett.* **1982**, *92*, 533-540.
(14) Chu, N. Y. C.; Kearns, D. R. *J. Phys. Chem.* **1970**, *74*, 1255-1260.
(15) Chandross, E. A.; Ferguson, J.; McRae, E. G. *J. Chem. Phys.* **1966**, *45*, 3546-3553.

Contribution from the Department of Chemistry, University of California, Berkeley, California 94720

EPR Spectroscopy of Mixed-Valence μ-Oxo-Bridged Manganese(III)/Manganese(IV) Porphyrin Complexes

Mark J. Camenzind, Bruce C. Schardt, and Craig L. Hill*

Received May 10, 1983

Several manganese ions in close proximity have been proposed to be present at the oxygen-evolving site of photosystem II.[1] The four-electron oxidation of water at this site may involve the cycling of the oxidation states of manganese ions that are bridged by oxygen ligands. The study of the interactions between manganese ions in synthetic complexes as they change oxidation states may improve the understanding of the interactions between the manganese ions in photosystem II.

We have previously reported the characterization of the oxo-bridged dimeric manganese(IV) porphyrin complexes $[(OCN)Mn^{IV}TPP]_2O$ and $[(N_3)Mn^{IV}TPP]_2O$, including a crystal and molecular structure determination for the latter complex.[2,3] The two manganese(IV) ions in each of these complexes are strongly antiferromagnetically coupled, making the complexes EPR silent.[3] The isolated complex $[(N_3)Mn^{IV}TPP]_2O$ has been shown to oxidize cyclohexane at room

* To whom correspondence should be addressed at Department of Chemistry, Emory University, Atlanta, GA 30322.

0020-1669/84/1323-1984$01.50/0